Article

Azobenzene-Linked Porphyrin–Fullerene Dyads

David I. Schuster, Ke Li, Dirk M. Guldi, Amit Palkar, Luis Echegoyen, Christopher Stanisky, R. James Cross, Marja Niemi, Nikolai V. Tkachenko, and Helge Lemmetyinen

J. Am. Chem. Soc., **2007**, 129 (51), 15973-15982 • DOI: 10.1021/ja074684n

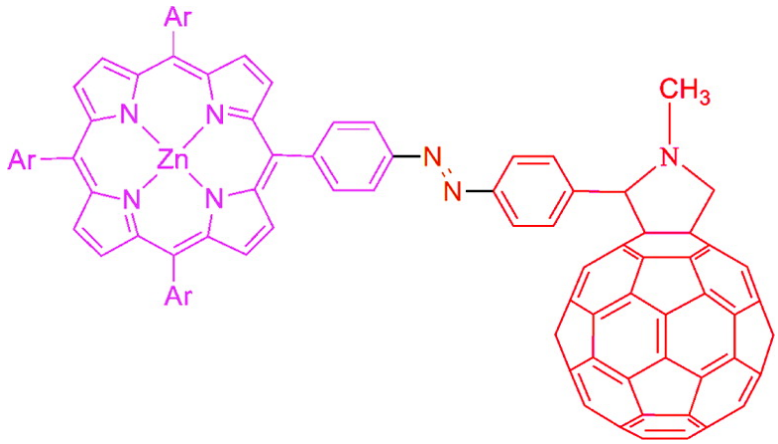

More About This Article

Additional resources and features associated with this article are available within the HTML version:

- Supporting Information
- Links to the 1 articles that cite this article, as of the time of this article download
- Access to high resolution figures
- Links to articles and content related to this article
- Copyright permission to reproduce figures and/or text from this article

View the Full Text HTML

J|A|C|S
ARTICLES
Published on Web 12/06/2007

Azobenzene-Linked Porphyrin−Fullerene Dyads

David I. Schuster,*,† Ke Li,†,‡ Dirk M. Guldi,*,§ Amit Palkar,|| Luis Echegoyen,|| Christopher Stanisky,⊥ R. James Cross,⊥ Marja Niemi,# Nikolai V. Tkachenko,# and Helge Lemmetyinen#

Contribution from the Chemistry Department, New York University, New York, New York 10003, Institute for Physical Chemistry, University of Erlangen, Erlangen 91085, Germany, Chemistry Department, Clemson University, Clemson, South Carolina 29634, Department of Chemistry, Yale University, New Haven, Connecticut 06520, and Institute of Materials Chemistry, Tampere University of Technology, 33101 Tampere, Finland

Received July 10, 2007; E-mail: david.schuster@nyu.edu

Abstract: A new group of porphyrin−fullerene dyads with an azobenzene linker was synthesized, and the photochemical and photophysical properties of these materials were investigated using steady-state and time-resolved spectroscopic methods. The electrochemical properties of these compounds were also studied in detail. The synthesis involved oxidative heterocoupling of free base tris-aryl-*p*-aminophenyl porphyrins with a *p*-aminophenylacetal, followed by deprotection to give the aldehyde, and finally Prato 1,3-dipolar azomethineylide cycloaddition to C_{60}. The corresponding Zn(II)-porphyrin (ZnP) dyads were made by treating the free base dyads with zinc acetate. The final dyads were characterized by their ^{1}H NMR, mass, and UV−vis spectra. ^{3}He NMR was used to determine if the products are a mixture of *cis* and *trans* stereoisomers, or a single isomer. The data are most consistent with the isolation of only a single configurational isomer, assigned to the *trans* (*E*) configuration. The ground-state UV−vis spectra are virtually a superimposition of the spectral features of the individual components, indicating there is no interaction of the fullerene (F) and porphyrin (H_2P/ZnP) moieties in the ground state. This conclusion is supported by the electrochemical data. The steady-state and time-resolved fluorescence spectra indicate that the porphyrin fluorescence in the dyads is very strongly quenched at room temperature in the three solvents studied: toluene, tetrahydrofuran (THF), and benzonitrile (BzCN). The fluorescence lifetimes of the dyads in all solvents are sharply reduced compared to those of H_2P and ZnP standards. In toluene, the lifetimes of the free base dyads are 600−790 ps compared to 10.1 ns for the standard, while in THF and BzCN the dyad lifetimes are less than 100 ps. For the ZnP dyads, the fluorescence lifetimes were 10−170 ps vs 2.1−2.2 ns for the ZnP references. The mechanism of the fluorescence quenching was established using time-resolved transient absorption spectroscopy. In toluene, the quenching process is singlet−singlet energy transfer ($k \approx 10^{11}$ s^{-1}) to give C_{60} singlet excited states which decay with a lifetime of 1.2 ns to give very long-lived C_{60} triplet states. In THF and BzCN, quenching of porphyrin singlet states occurs at a similar rate, but now by electron transfer, to give charge-separated radical pair (CSRP) states, which show transient absorption spectra very similar to those reported for other H_2P−C_{60} and ZnP−C_{60} dyad systems. The lifetimes of the CSRP states are in the range 145−435 ns in THF, much shorter than for related systems with amide, alkyne, silyl, and hydrogen-bonded linkers. Thus, both forward and back electron transfer is facilitated by the azobenzene linker. Nonetheless, the charge recombination is 3−4 orders of magnitude slower than charge separation, demonstrating that for these types of donor−acceptor systems back electron transfer is occurring in the Marcus inverted region.

1. Introduction

Studies on photoinduced interactions between porphyrin and fullerenes have provided important methods for developing new materials for molecular optoelectronics.[1] Since fullerene[60] is an excellent electron acceptor,[2] it is considered to be one of the most important components for new types of electron donor−acceptor (D−A) systems.[3] With this objective, a large number of covalently linked porphyrin/fullerene (P−F) and related multichromophoric systems have been synthesized, and

† New York University.
‡ Current address: Central Research and Development, E. I. DuPont de Nemours and Co., Experimental Station, Wilmington, DE 19880.
§ University of Erlangen.
|| Clemson University.
⊥ Yale University.
Tampere University of Technology.

(1) *Fullerenes, From Synthesis to Optoelectronic Properties*; Guldi, D. M., Martin, N., Eds.; Kluwer Academic Publishers: Dordrecht, 2002.
(2) For comprehensive reviews, see: (a) Echegoyen, L.; Echegoyen, L. E. *Acc. Chem. Res.* **1998**, *31*, 593. (b) Opallo, M. *Pol. J. Chem.* **1993**, *67*, 2093. (c) Fukuzumi, S. *Res. Chem. Intermed.* **1997**, *23*, 519.
(3) (a) Kadish, K. M., Ruoff, R. M., Eds. *Fullerenes: Chemistry, Physics and Technology*; Wiley-Interscience: New York, 2000. (b) Guldi, D. M. *Chem. Soc. Rev.* **2002**, *31*, 22 and references therein. (c) Figueira-Duarte, T. M.; Gegout, A.; Nierengarten, J. F. *Chem. Commun.* **2007**, 109.

their photophysical properties have been thoroughly investigated.[4,5] Recently, there have been several studies on mechanically linked systems in which these chromophores were incorporated into rotaxane and catenane architectures.[6] These fullerene-based systems show an inhibition to back electron transfer upon photoexcitation, resulting in long-lived charge-separated states. These studies have contributed significantly to progress in the development of artificial photosynthetic systems[7] and organic solar cells.[8]

Azobenzene is a well-studied photoresponsive system that can undergo *cis*/*trans* isomerization under irradiation with UV−vis light.[9] While there has been one study of electron-rich and electron-deficient porphyrin groups linked by an azobenzene unit,[10] and fullerene−azobenzene (**C_{60}−Az**) derivatives have been synthesized and studied,[11] there has been no report until now on porphyrin−azobenzene−fullerene (**P−Az−C_{60}**) hybrid systems. Linkage of P and C_{60} moieties to a central azobenzene moiety generates novel dyads whose behavior upon photoexcitation can be controlled directly by the linker rather than by the auxiliaries, potentially inducing novel photophysical properties.

Herein we report the first synthesis, electrochemical and photophysical study of **P−Az−C_{60}** hybrid systems. We anticipated that such materials would exhibit different photophysical properties in its *cis (Z)* and *trans (E)* configurations. The structures of the new azobenzene-linked pophyrin−fullerene dyads synthesized in this study, including both free base (H_2P) and ZnP moieties, are shown in Scheme 1. The systems were designed so that the only structural change resulting from UV−vis irradiation would be isomerization around the central N═N bond.

1.1. Synthesis. The synthesis of the new dyads is summarized in Scheme 1. The convergent approach that was previously used for synthesis of azo-linked porphyrin dimers[10] could not be used due to the incompatibility of C_{60} derivatives with the strongly basic conditions used in that study. Instead, oxidative heterocoupling of free base aminoporphyrins **1** (Ar = *p*-tolyl or 3,5-di-*tert*-butylphenyl)[12] and aminoacetal **2**[13] using MnO_2 as the oxidant[14] was utilized. This coupling reaction proceeded smoothly in toluene under reflux for 12 h to give **3**. After deprotection of the acetals using trifluoroacetic acid (TFA) in a mixture of CH_2Cl_2 and water at room temperature for 8 h, the free base porphyrin aldehydes were treated with C_{60} and sarcosine (*N*-methylglycine) in refluxing toluene for 6 h to give **H_2P−Az−C_{60}** dyads **4a** (Ar = *p*-tolyl) and **4b** (Ar = 3,5-di-*tert*-butylphenyl) in ∼50% yield via a 1,3-dipolar azomethineylide cycloaddition reaction.[15] Dyads **4a** and **4b** were then converted using zinc acetate into the corresponding zinc porphyrin dyads **5a** and **5b**, **ZnP−Az−C_{60}**.

The structures of these dyads were verified by ^{1}H NMR, ^{3}He NMR, UV−vis, and MALDI-TOF mass spectroscopy (see Experimental Section for details).

1.2. The UV−Vis Absorption Spectra of these donor−acceptor hybrids are best described as simple superimpositions of the spectra of the individual components, lacking notable perturbations or additional charge-transfer transitions. In particular, the dominating Soret- and Q-bands of the porphyrins are seen at 420 nm and 550−650 nm, respectively. The strongest bands due to C_{60}, on the other hand, are at 220, 265, and 330

(4) (a) Martin, N.; Sanchez, L.; Illescas, B.; Perez, I. *Chem. Rev.* **1998**, *98*, 2527. (b) Prato, M.; Maggini, M. *Acc. Chem. Res.* **1998**, *31*, 519. (c) Imahori, H.; Shunichi, F. *Adv. Funct. Mater*. **2004**, *14*, 525.

(5) For reviews, see: (a) Guldi, D. M. *Chem. Commun.* **2000**, 321. (b) Thomas, K. G.; George, M. V.; Kamat, P. V. *Helv. Chim. Acta* **2005**, *88*, 1291. For recent examples of P-F systems, see: (c) Imahori, H.; Sekiguchi, Y.; Kashiwagi, Y.; Sato, T.; Araki, Y.; Ito, O.; Yamada, H.; Fukuzumi, S. *Chem. Eur. J.* **2004**, *10*, 3184. (d) Imahori, H. *Org. Biomol. Chem.* **2004**, *2*, 1425. (e) Guldi, D. M.; Imahori, H.; Tamaki, K.; Kashiwagi, Y.; Yamada, H.; Sakata, Y.; Fukuzumi, S. *J. Phys. Chem. A* **2004**, *108*, 541. (f) Tkachenko, N. V.; Lemmetyinen, H.; Sonoda, J.; Ohkubo, K.; Sato, T.; Imahori, H.; Fukuzumi, S. *J. Phys. Chem. A* **2003**, *107*, 8834−8844. (g) Ohkubo, K.; Imahori, H.; Shao, J.; Ou, Z.; Kadish, K. M.; Chen, Y.; Zheng, G.; Pandey, R. K.; Fujitsuka, M.; Ito, O.; Fukuzumi, S. *J. Phys. Chem. A* **2002**, *106*, 10991. (h) Kesti, T. J.; Tkachenko, N. V.; Vehmanen, V.; Yamada, H.; Imahori, H.; Fukuzumi, S.; Lemmetyinen, H. *J. Am. Chem. Soc.* **2002**, *124*, 8067. (i) Imahori, H.; Tamaki, K.; Araki, Y.; Sekiguchi, Y.; Ito, O.; Sakata, Y.; Fukuzumi, S. *J. Am. Chem. Soc.* **2002**, *124*, 5165. (j) Imahori, H.; Tamaki, K.; Araki, Y.; Hasobe, T.; Ito, O.; Shimomura, A.; Kundu, S.; Okada, T.; Sakata, Y.; Fukuzumi, S. *J. Phys. Chem. A* **2002**, *106*, 2803. (k) Fukuzumi, S.; Ohkubo, K.; Imahori, H.; Shao, J.; Ou, Z.; Zheng, G.; Chen, Y.; Pandey, R. K.; Fujitsuka, M.; Ito, O.; Kadish, K. M. *J. Am. Chem. Soc.* **2001**, *123*, 10676. (l) Imahori, H.; Guldi, D. M.; Tamaki, K.; Yoshida, Y.; Luo, C.; Sakata, Y.; Fukuzumi, S. *J. Am. Chem. Soc.* **2001**, *123*, 6617. (m) Imahori, H.; Tamaki, K.; Guldi, D. M.; Luo, C.; Fujitsuka, M.; Ito, O.; Sakata, Y.; Fukuzumi, S. *J. Am. Chem. Soc.* **2001**, *123*, 2607. (n) Imahori, H.; Tkachenko, N. V.; Vehmanen, V.; Tamaki, K.; Lemmetyinen, H.; Sakata, Y.; Fukuzumi, S. *J. Phys. Chem. A* **2001** *105*, *1750*. (o) Imahori, H.; El-Khouly, M. E.; Fujitsuka, M.; Ito, O.; Sakata, Y.; Fukuzumi, S. *J. Phys. Chem. A* **2001**, *105*, 325.

(6) From our group: (a) Schuster, D. I.; Li, K.; Guldi, D. M. *C. R. Chimie* **2006**, *9*, 892. (b) Li, K.; Bracher, P. J.; Guldi, D. M.; Herranz, M. A.; Echegoyen, L.; Schuster, D. I. *J. Am. Chem. Soc.* **2004**, *126*, 9156. (c) Schuster, D. I.; Li, K.; Guldi, D. M.; Ramey, J. *Org. Lett.* **2004**, *6*, 1919. (d) Li, K.; Schuster, D. I.; Guldi, D. M.; Herranz, M. A.; Echegoyen, L. *J. Am. Chem. Soc.* **2004**, *126*, 3388. From Ito's group: (e) Watanabe, N.; Kihara, N.; Furusho, Y.; Takata, T.; Araki, Y.; Ito, O. *Angew. Chem., Int. Ed*. **2005**, *42*, 681. (f) Sandanayaka, A. S. D.; Watanabe, N.; Ikeshita, K.-I.; Araki, Y.; Kihara, N.; Furusho, Y.; Ito, O.; Takata, T. *J. Phys. Chem. B* **2005**, *109*, 2516. (g) Sandanayaka, A. S. D.; Ikeshita, K.-I.; Watanabe, N.; Araki, Y.; Furusho, Y.; Kihara, N.; Takata, T.; Ito, O. *Bull. Chem. Soc. Japan* **2005**, *78*, 1008. (h) Sandanayaka, A. S. D.; Sasabe, H.; Araki, Y.; Furusho, Y.; Ito, O.; Takata, T. *J. Phys. Chem. A* **2004**, *108*, 5145. (i) Rajkumar, G. A.; Sandanayaka, A. S. D.; Ikeshita, K.-I.; Araki, Y.; Furusho, Y.; Takata, T.; Ito, O. *J. Phys. Chem. B* **2006**, *110*, 6516. (j) Sasabe, H.; Furusho, Y.; Sandanayaka, A. S. D.; Araki, Y.; Kihara, N.; Mizuno, K.; Ogawa, A.; Takata, T.; Ito, O. *J. Porphyrins Phthalocyanines* **2006**, *10*, 1346. (k) Maes, M.; Sasabe, H.; Kihara, N.; Araki, Y.; Furusho, Y.; Mizuno, K.; Takata, T.; Ito, O. *J. Porphyrins Phthalocyanines* **2005**, *9*, 724. From Nierengarten's group: (l) Armaroli, N.; Diederich, F.; Dietrich-Buchecker, C. O.; Flamigni, L.; Marconi, G.; Nierengarten, J.-F.; Sauvage, J.-P. *Chem. Eur. J.* **1998**, *4*, 406. (m) Clifford, J. N.; Accorsi, G.; Cardinali, F.; Nierengarten, J.-F.; Armaroli, N. *C. R. Chimie* **2006**, *9*, 1005.

(7) (a) Liddell, P. A.; Kodis, G.; Andreasson, J.; de la Garza, L.; Bandyopadhyay, S.; Mitchell, R. H.; Moore, T. A.; Moore, A. L.; Gust, D. *J. Am. Chem. Soc.* **2004**, *126*, 4803. (b) Liddell, P. A.; Kodis, G.; Moore, A. L.; Moore, T. A.; Gust, D. *J. Am. Chem. Soc.* **2002**, *124*, 7668. For a recent excellent review in this field, see: (c) Flamigni, L.; Heitz, V.; Sauvage, J.-P. *Struct. Bonding* **2006**, *121*, 217.

(8) For examples, see: Imahori, H; Sakata, Y. *Adv. Mat.* **1997**, *9*, 537; Hasobe, T.; Imahori, H.; Kamat, P. V.; Fukuzumi, S. *J. Am. Chem. Soc.* **2003**, *125*, 14962; Imahori, H.; Kashiwagi, Y.; Hasobe, T.; Kimura, M.; Hanada, T.; Nishimura, Y.; Yamazaki, I.; Araki, Y.; Ito, O.; Fukuzumi, S. *Thin Solid Films* **2004**, *451*, 580; Guldi, D. M.; Aminur Rahman, G. M.; Sgobba, V.; Ehli, C. *Chem. Soc. Rev.* **2006**, *325*, 471; Segura, J. L.; Martin, N.; Guldi, D. M. *Chem. Soc. Rev.* **2005**, *324*, 31; Marczak, R.; Sgobba, V.; Kutner, W.; Gadde, S.; D'Souza, F. D.; Guldi, D. M. *Langmuir* **2007**, *23*, 1917; Nava, M. G.; Setayesh, S.; Rameau, A.; Masson, P.; Nierengarten, J.-F. *New J. Chem.* **2002**, *26*, 1584; Nierengarten, J.-F. *New J. Chem.* **2004**, *28*, 1177. Backer, S. A.; Sivula, K.; Kavulak, D. F.; Frechét, J. M. J. Chem. Materials **2007**, *19*, 2927.

(9) (a) Helmut, K. *CRC Handbook of Organic Photochemistry and Photobiology*, 2nd ed.; CRC Press: Boca Raton, FL, 2004; pp 1−89. (b) For a leading reference for azobenzene-controlled complex, see: Muraoka, T.; Kinbara, K.; Aida, T. *Nature* **2006**, *440*, 512. (c) For a comprehensive review of azobenzene-containing supramolecular systems, see: Balzani, V.; Credi, A.; Raymo, F. M.; Stoddart, J. F. *Angew. Chem., Int. Ed.* **2000**, *39*, 3348 and references therein.

(10) Tsuchiya, S. *J. Am. Chem. Soc*. **1999**, *121*, 48.

(11) (a) Kay, K.-Y.; Han, K.-J.; Yu, Y.-J.; Park, Y.-D. *Tetrahedron Lett.* **2002**, *43*, 5053. (b) Oh-ishi, K.; Okamura, J.; Ishi-I, T.; Sano, M.; Shinkai, S. *Langmuir* **1999**, *15*, 2224.

(12) Imahori, H.; Hagiwara, K.; Aoki, M.; Akiyama, T.; Taniguchi, S.; Okada, T.; Shirakawa, M.; Sakata, Y. *J. Am. Chem. Soc.* **1996**, *118*, 11771.

(13) Imahori, H.; Tamaki, K.; Yamada, H.; Yamada, K.; Sakata, Y.; Nishimura, Y.; Yamazaki, I.; Fujitsuka, M.; Ito, O. *Carbon* **2000**, *38*, 1599.

(14) For MnO_2-mediated homocoupling synthesis of azobenzene derivatives, see: Pratt, E. F.; McGovern, T. P. *J. Org. Chem.* **1964**, *29*, 1540. For a recent report of a molecular hinge of azobenzene derivatives using a MnO_2-mediated synthesis, see: Norikane, Y.; Tamaoki, N. *Org. Lett.* **2004**, *6*, 2595.

(15) Maggini, M.; Scorrano, G.; Prato, M. *J. Am. Chem. Soc*. **1993**, *115*, 9798.

Scheme 1. Synthesis of Porphyrin−Azobenzene−Fullerene Dyads

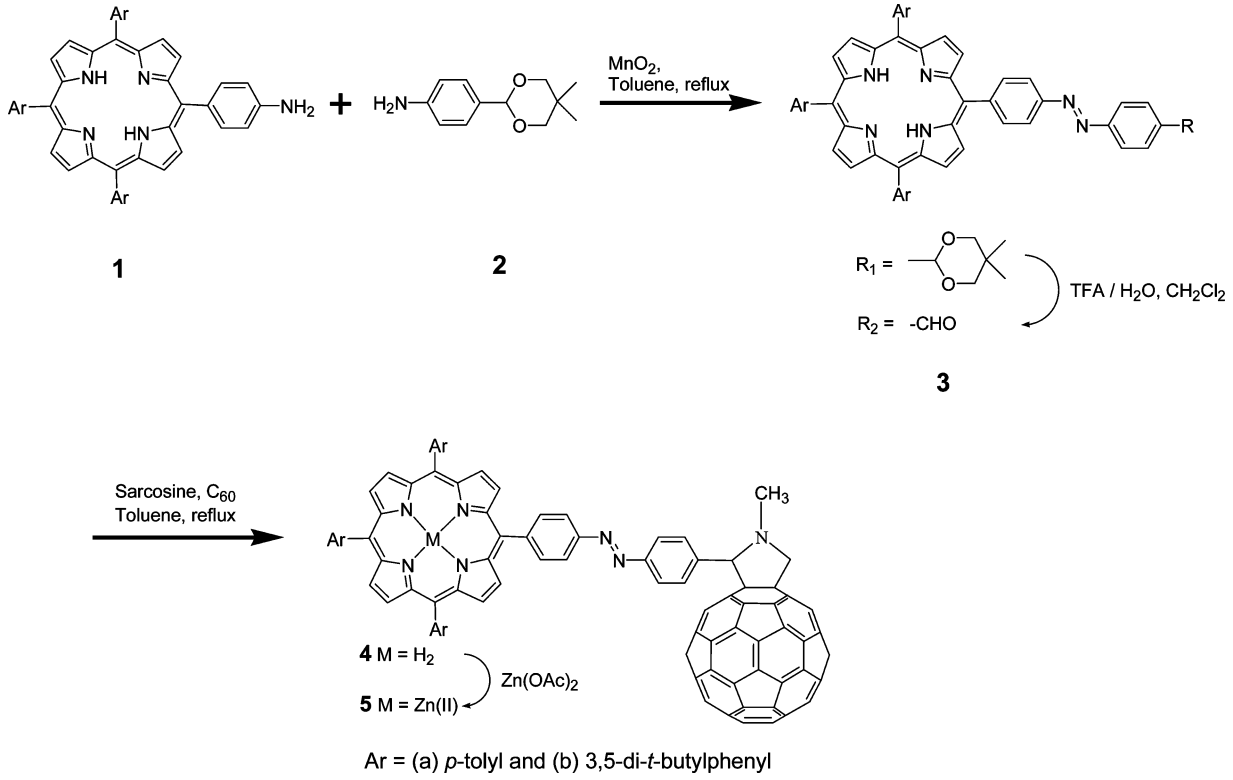

nm and extend all the way to the energetically lowest-lying transition at 690 nm (see Figure 1). The lack of interchromophoric interaction in the ground state is in accord with the large donor−acceptor separations of 14−15 Å, which also prevents demonstrable interactions in similarly spaced donor−acceptor ensembles.[4−6]

1.3. ^{3}He NMR Studies. An important structural concern was whether the synthesized dyads **4** and **5** were mixtures of *cis* (*Z*) and *trans (E*) isomers or were single stereoisomers. The sharpness of the ^{1}H NMR spectra of the isolated dyads suggested that they were mostly, if not entirely, composed of a single configurational isomer (see Figure S19, Supporting Information, for the ^{1}H NMR spectrum of **4a**). We decided to confirm this experimentally using ^{3}He NMR studies on materials prepared from C_{60} containing an endohedral ^{3}He atom ($I = {}^1/_2$) (^{3}He@C_{60}). Cross, Saunders, and co-workers at Yale have shown that ^{3}He spectra of derivatives of ^{3}He@C_{60} provide information about the number and nature of the products formed, including stereoisomers.[16] The NYU and Yale teams have collaborated several times on such studies, including distinction between C_{60}−pyrrolidine and C_{60}−malonate bis-adducts.[17] In the present case, the best ^{3}He NMR spectra were obtained for dyad **4b** with *tert*-butyl substituents on the aromatic porphyrin substituents. After 4 h acquisition time, the spectrum of **4b** (see Figure S15, Supporting Information) showed only a single peak at −9.7 ppm (relative to ^{3}He gas at 0.0 ppm, and ^{3}He@C_{60} at −6.3 ppm; all experiments were performed using 1-methylnaphthalene as solvent), although a second peak at −9.3 ppm appeared after 10,000 scans (11 h). For the *p*-tolyl dyad **4a**, the corresponding peaks appear at −10.3 and −9.5 ppm. The problem is that the spectra were not reproducible with respect to the lower-field peaks, particularly on samples which had been stored for several weeks. Thus, we are not certain if the lower-field peaks are due to a second configurational isomer or to some decomposition product. We favor the second explanation, as there is evidence from spectroscopic studies that these azo-linked dyads are thermally unstable upon extended storage, but the nature of the decomposition products has not been studied.

1.4. Electrochemistry. For electrochemical measurements on compounds **3**, **4a**, **4b**, **5a**, and **5b**, 0.1 M tetrabutylammonium hexafluorophosphate ($TBAPF_6$, from Fluka) in anhydrous CH_2Cl_2 was used as the supporting electrolyte (degassed with argon saturated with CH_2Cl_2 vapors). A platinum wire was employed as the counter electrode, and a nonaqueous Ag/AgCl electrode was used as the reference. Ferrocene (Fc) was added as an internal reference, and all the potentials were referenced relative to the Fc/Fc$^+$ couple. A glassy carbon electrode (CHI, 1.5 mm in diameter), polished with 0.3 μm aluminum paste and ultrasonicated in deionized water and CH_2Cl_2 bath, was used as the working electrode. The scan rate for cyclic voltammetry (CV) was 100 mV/s, whereas for differential pulse voltammetry (DPV) the pulse rate was 0.05 s at increments of 4 mV and amplitude of 50 mV. Experiments were performed at room temperature (20 ± 2 °C). All potentials obtained from DPV

(16) (a) Saunders, M.; Jiménez-Vázquez, H. A.; Cross, R. J.; Mroczkowski, S.; Freedberg, D. I.; Anet, F. A. L. *Nature* **1994** *367*, 256; Saunders, M.; Jiménez-Vázquez, H. A.; Bangerter, B. W.; Cross, R. J.; Mroczkowski, S.; Freedberg, D. I.; Anet, F. A. L. *J. Am. Chem. Soc.* **1994**, *116*, 3621; Saunders, M.; Jiménez-Vázquez, H. A.; Cross, R. J.; Billups, W. E.; Gesenberg, C.; Gonzalez, A.; Luo, W.; Haddon, R. C.; Diederich, F.; Herrmann, Z. *J. Am. Chem. Soc.* **1995**, *117*, 9305; Rüttimann, M.; Haldimann, R. F.; Isaacs, L.; Diederich, F.; Khong, A.; Jiménez-Vázquez, H. A.; Cross, R. J.; Saunders, M. *Chem. Eur. J.* **1997**, *3*, 1071.

(17) For leading references, see: (a) Cross, R. J.; Jimenez-Vazquez, H. A.; Lu, Q.; Saunders, M.; Schuster, D. I.; Wilson, S. R.; Zhao, H. *J. Am. Chem. Soc.* **1996**, *118*, 11454. (b) Wilson, S. R.; Yurchenko, M. E.; Schuster, D. I.; Khong, A.; Saunders, M. *J. Org. Chem.* **2000**, *65*, 2619. (c) Rosenthal, J.; Schuster, D. I.; Cross, R. J.; Khong, A. M. *J. Org. Chem.* **2006**, *71*, 1191.

Table 1. Electrochemical Data on Porphyrin−Fullerene Dyads and Reference Compounds[a]

CV potentials

	oxidation				reduction			
cmpd	*E*1	*E*2	*E*1	*E*2	*E*3	*E*4	*E*5	*E*6
NMFP[d]	0	0	−1.1		−1.48			−2.01
3	0.55	0.83				−1.65		−2.00[c]
4a	0.52	0.83	−1.09		−1.46	−1.64		−2.06[c]
5a	0.35	0.66	−1.07		−1.44		−1.78	−1.99[c]
4b	0.58	NO[b]	−1.06		−1.44	−1.65		−1.99[c]
5b	0.34	0.69	−1.07		−1.45		−1.82	−1.99[c]

DPV potentials

	oxidation				reduction			
cmpd	*E*1	*E*2	*E*1	*E*2	*E*3	*E*4	*E*5	*E*6
3	0.56	0.84				−1.64		−1.99
4a	0.53	0.84	−1.07		−1.45	−1.62		−2.01
5a	0.34	0.65	−1.07		−1.44		−1.77	−2.00
4b	0.56	0.85	−1.05		−1.43	−1.64		−1.99
5b	0.30	0.70	−1.06		−1.44		−1.82	−1.98

[a] All the potentials, in volts, were measured relative to the F_c/F_c^+ couple. [b] Indicates not observed. [c] Indicates irreversible peaks. [d] *N*-methylfulleropyrrolidine.

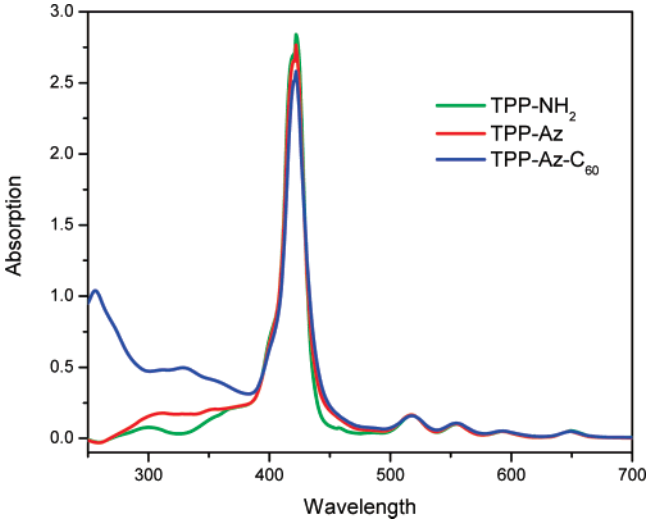

Figure 1. UV−vis absorption spectrum of **4a** and reference materials in dichloromethane.

were converted to $E_{1/2}$ values using the formula $E_{max} = E_{1/2} + \Delta E/2$, where ΔE is the pulse amplitude.[18]

Measurements were first performed on reference compound **3** which has a porphyrin core and the azobenzene spacer but no fulleropyrrolidine moiety. The cyclic voltammogram (CV) and differential pulse voltammogram (DPV) of compound **3** are shown in Figures S1and S2 (Supporting Information). The observed potentials are given in Table 1. In DPV, compound **3** shows two reversible oxidation waves, at +0.56 and at +0.84 V, while two reduction waves are observed at −1.64 and −1.99 V. These potentials compare well with those of other model free base porphyrins.[18] The CV of **3** shows similar characteristics.

Figure 2 shows the DPV of compound **4a**. The compound shows four reduction processes at −1.07, −1.45, −1.62, and −2.01 V, respectively (see Table 1). Similar values are seen in

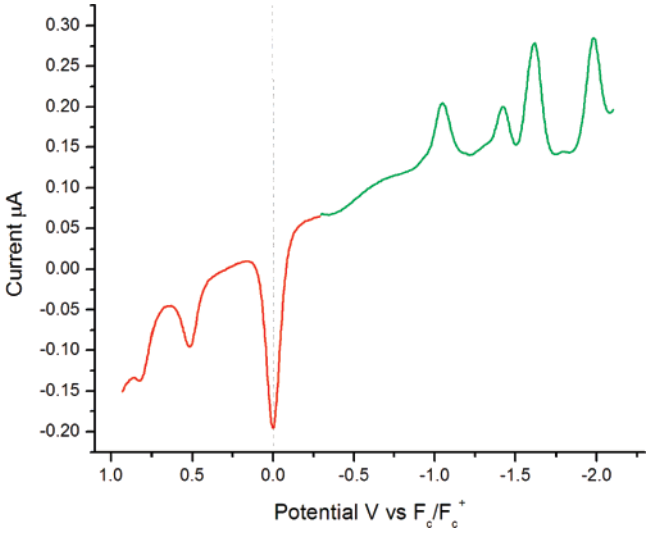

Figure 2. Differential pulse voltammagram of compound **4a**.

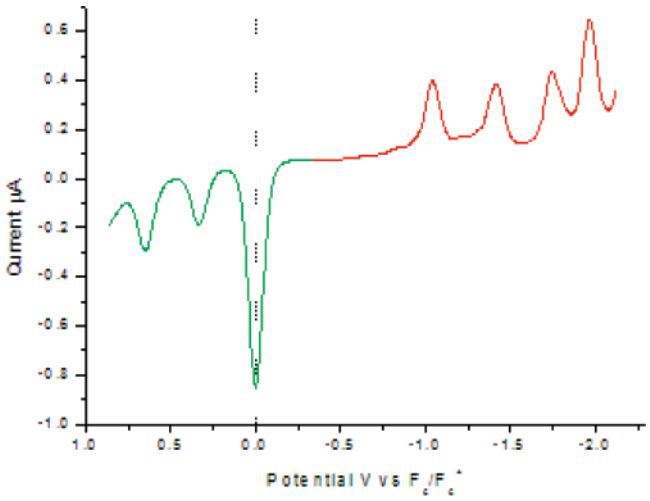

Figure 3. Differential pulse voltammagram of compound **5a**.

the CV (Figure S7, Supporting Information). It has been shown that *N*-methylfulleropyrrolidine (NMFP) has first and second reduction potentials around −1.1 V and −1.5 V, respectively.[15,20] The first and the second reductions thus correspond to the fulleropyrrolidine unit, while the third appears to be centered on the porphyrin, based on the values obtained for reference compound **3**. The last reduction could be a multiple electron reduction of the fullerene and porphyrin-spacer moieties as the potential corresponds well with the third reduction of the fulleropyrrolidine as well as the second reduction of porphyrin. The first oxidation potential is at +0.53 V (DPV) which is in good agreement with the potential observed for the reference porphyrin **3**. The smaller oxidation peaks at ∼0.8 eV, also seen with **3**, are attributed to formation of porphyrin dications. The DPV of compound **4a** is a superimposition of the DPVs of the individual fulleropyrrolidine and porphyrin-spacer units. Similar results were obtained from the CV (Figure S7, Supporting Information).

(18) Electrochemical method: Bard, A. J.; Faulkner, L. R. *Electrochemical Methods: Fundamentals and Applications*, 2nd. ed.; John Wiley and Sons: New York, 2001.

(19) Beavington, R.; Burn, P. L. *J. Chem. Soc., Perkin. Trans. 1* **2000**, *8*, 1231. For electrochemical data of porphyrins, see: Kadish, K. M., Smith, K. M., Guilard, R., Eds. *The Porphyrin Handbook*; Academic Press: San Diego, 1999; Vol. 9.

(20) Tat, F. T.; Zhou, Z.; MacMahon, S. A.; Song, F.; Rheingold, A. L.; Echegoyen, L.; Schuster, D. I.; Wilson, S. R. *J. Org. Chem.* **2000**, *69*, 4602.

The potentials obtained from the DPV as well as the CV of the corresponding zinc complex **5a** show a behavior similar to that of the free base analogue **4a**. Compound **5a** shows two oxidation and four reduction processes in DPV as shown in Figure 3 (for the CV of **4a** and **5a**, see Figures S7 and S8, Supporting Information). Both oxidation potentials are shifted cathodically relative to those of **4a**, by 210 and 190 mV, respectively, due to the presence of the zinc atom inside the porphyrin. The corresponding shifts in the CV are 170 mV. The first and the third reduction processes at −1.07 and −1.44 V in the DPV correspond well with the fullerene peaks seen for **4a**. The third peak for **5a** at −1.77 V could not be attributed to either the fullerene or the azobenzene moieties. However, zinc tetraphenylporphine has its first reduction potential at ∼−1.8 V,[22] indicating that the third reduction peak in the dyads is porphyrin-centered. The fourth reduction observed in the DPV at −2.00 V for **5a** (−1.99 V in the CV) is attributed to a combination of fullerene and porphyrin moieties. Thus, the zinc affects the oxidation and reduction potentials of the porphyrin moiety but not of the fullerene. As indicated, the potentials obtained from the DPV match those obtained from the CV studies very well.

The electrochemical properties of homologous dyads **4b** and **5b** (see Figures S3−S6, Supporting Information) are very similar to those of **4a** and **5a**. The data for all five compounds studied are compiled in Table 1.

1.5. Photophysics. 1.5.1. Fluorescence Spectroscopy. Decays of the fluorescence at 605 and 660 nm, corresponding to the maxima in the fluorescence of ZnP and H_2P, respectively, were measured at Erlangen following excitation at 550 nm. The fluorescence decay curves of the references were best fitted by a single-exponential decay law. For ZnP the lifetimes were 2.14 ns (toluene), 2.2 ns (THF), and 2.08 ns (BzCN), while the H_2P fluorescence lifetime of 10.1 ns in did not change with solvent polarity.

To study the electronic interactions between the porphyrin and fullerene π-systems in the excited state, emission measurements were carried out with the **ZnP−Az−C_{60}** and **H_2P−Az−C_{60}** systems in solvents of different polarity (toluene, THF, and benzonitrile (BzCN)). The data are compared with ZnP and H_2P references which lack the electron-accepting C_{60} moiety. The ^{1}ZnP* and ^1H_2P* emission is significantly quenched in all solvents with quantum yields (Φ) that range from 0.0001 to 0.017 (for details see Table 2). Figures 4 and 5 illustrate the fluorescence trends in THF and BzCN as solvents. For the corresponding ZnP and H_2P references the fluorescence quantum yields are 0.04 and 0.15, respectively. Although the yields are reduced in the dyads, the emission patterns of ZnP and H_2P are not affected by the presence of the C_{60} moiety.

Table 2. Photophysical Data for Dyads in Several Solvents at Room Temperature

solvent	4a	4b	5a	5b
		fluorescence quantum yields		
toluene	0.011	0.017	0.0005	0.0026
THF	0.004	0.005	0.0002	0.0013
BzCN	0.0015	0.003	0.0001	0.0010
		k_{et}, [s^{-1}][a]		
toluene	1.2×10^9,[b]	7.8×10^9,[b]	3.9×10^{10},[b]	7.2×10^9,[b]
THF	3.7×10^9	2.9×10^9	9.9×10^{10}	1.5×10^{10}
BzCN	9.9×10^9	4.9×10^9	1.9×10^{11}	2.0×10^{10}
		fluorescence lifetime, ns		
toluene	0.60 (0.63)[e]	0.79 (0.52)[e]	*d*	0.11
THF	0.16	0.19	*d*	*d*
BzCN	0.16 [e]	0.19 [e]	*d*	*d*
		singlet excited−state lifetime, ns		
toluene	0.56	0.72	0.04	0.10
THF	0.15	0.17	0.02	0.05
BzCN	0.09	0.13	0.01	0.02
		k_{et},[s^{-1}][c]		
toluene	1.6×10^9,[b]	1.3×10^9,[b]	2.5×10^{10}	9.5×10^9
THF	6.5×10^9	5.7×10^9	5.0×10^{10}	2.0×10^{10}
BzCN	1.0×10^{10}	7.5×10^9	1.0×10^{11}	5.0×10^{10}
		charge-separated radical pair lifetime, ns		
THF	175	435	145	290
BzCN	0.66[e]	1.2 [e]	−	−

[a] Calculated using eq 1 from fluorescence lifetime data. [b] Rates of singlet−singlet energy transfer; see text. [c] Calculated using eq 2 from femtosecond transient absorption data. [d] Could not be determined due to the instrumental resolution of instrumentation at Erlangen of 0.1 ns. [e] Experiments done at Tampere.

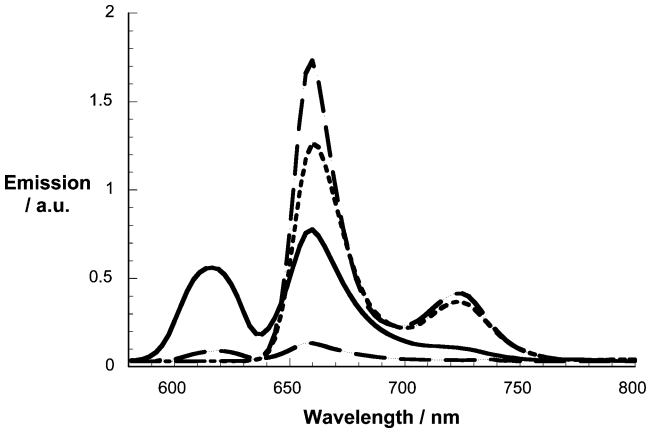

Figure 4. Room-temperature fluorescence spectra of ***tert*-Bu-ZnP−C_{60} (5b)** (solid), **Me-ZnP−C_{60} (5a)** (short dashed), ***tert*-Bu-H_2P−C_{60} (4b)** (long dashed), and **Me−H_2P−C_{60} (4a)** (dotted) in THF recorded on solutions with optical density 0.5 at the 425 nm excitation wavelength.

A closer inspection of the fluorescence data reveals a number of interesting features. First, upon changing the solvent polarity from toluene ($\epsilon = 2.38$) to THF ($\epsilon = 7.6$) to benzonitrile ($\epsilon = 24.8$) a gradual intensification of the quenching is discernible for all **ZnP−C_{60}** and **H_2P−C_{60}** systems. Better solvation of charged species in polar media results in (i) lower energies of the radical ion pair states and (ii) larger energy gaps relative to the photoexcited porphyrin state. Thus, we attribute the trend in quenching as a function of solvent polarity to intramolecular charge transfer, which is mediated through the azobenzene-connecting bridge and facilitated by larger thermodynamic driving forces.

Second, appreciably stronger fluorescence quenching is noted for the **ZnP−C_{60}** systems *vis a vis* analogous **H_2P−C_{60}**

(21) Quantum yield reference: Murov, S. L.; Carmichael, I.; Hug, G. L. In *Handbook of Photochemistry*; Murov, S., Carmichael, I., Hug, G. L., Eds.; Marcel Dekker: New York, 1993.

(22) (a) Guldi, D. M.; Nuber, B.; Bracher, P. J.; Alabi, C. A.; MacMahon, S.; Kukol, J. W.; Wilson, S. R.; Schuster, D. I. *J. Phys. Chem. A* **2003**, *107*, 3215. (b) Schuster, D. I.; Cheng, P.; Jarowski, P. D.; Guldi, D. M.; Luo, C.; Echegoyen, L.; Pyo, S.; Holzwarth, A. R.; Braslavsky, S. E.; Williams, R. M.; Klihm, G. *J. Am. Chem. Soc.* **2004**, *126*, 7257. (c) Vail, S. A.; Krawczuk, P. J.; Guldi, D. M.; Palkar, A.; Echegoyen, L.; Tomé, J .P. C.; Fazio, M. A.; Schuster, D. I. *Chem. Eur. J.* **2005**, *11*, 3375. (d) Schuster, D. I.; MacMahon, S.; Guldi, D. M.; Echegoyen, L.; Braslavsky, S. E. *Tetrahedron* **2006**, *62*, 1928. (e) Vail, S. A.; Schuster, D. I.; Guldi, D. M.; Isosomppi, M.; Tkachenko, N.; Lemmetyinen, H.; Palkar, A.; Echegoyen, L.; Chen, X.; Zhang, J. Z. H. *J. Phys. Chem. B* **2006**, *110*, 14155. (f) Schuster, D. I. *Carbon* **2000**, *38*, 1607.

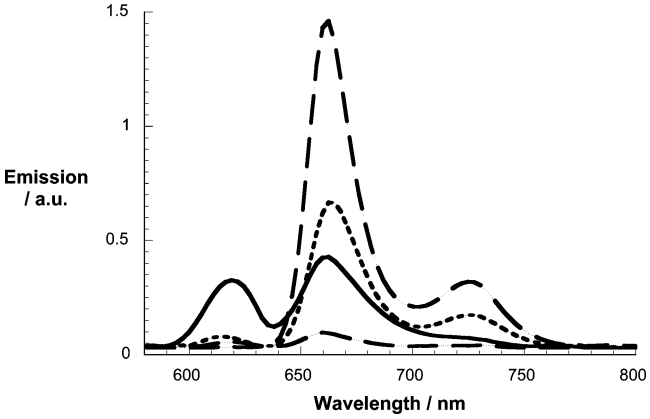

Figure 5. Room-temperature fluorescence spectra of ***tert*-Bu-ZnP−C_{60}** (**5b**) (solid), **Me-ZnP−C_{60}** (**5a**) (short dashed), ***tert*-Bu-H_2P−C_{60}** (**4b**) (long dashed), and **Me-H_2P−C_{60}** (**4a**) (dotted) in benzonitrile recorded on solutions with optical density 0.5 at the 425 nm excitation wavelength.

materials. In both systems, the methyl-substituted dyads exhibit faster deactivation. These trends are consistent with the electron donor characteristics of the porphyrins, which impact the energetics of the radical ion pair states. Thus, the ZnP oxidations are ca. 0.2 V easier than oxidation of the corresponding H_2P systems. For the free base dyads, substitution of methyl vs *tert*-butyl on the aryl ring lowers the first oxidation potential by 60 mV, while for the ZnP dyads the oxidation potential differences are the same within experimental error (see Table 1).

Third, for the **ZnP−Az−C_{60}** systems in toluene, the fullerene fluorescence signature was observed upon amplification of the 700−750 nm region. The fluorescence quantum yield of $5.0 \pm 0.5 \times 10^{-4}$ indicates high (at least 85%) transduction of singlet excitation, i.e., funneling of the singlet excitation from the ZnP chromophore (2.1 eV) to C_{60} (1.76 eV). Although the fullerene fluorescence appears only as a weak shoulder, it is noteworthy that in the more polar solvents, where electron transfer dominates, this feature entirely disappears. For the **H_2P−C_{60}** systems, such an analysis was impossible, due to the overlapping fluorescence of H_2P and C_{60} in the 700−750 nm region.

Relating the fluorescence quantum yields in the donor−acceptor ensemble, $\Phi_{(dyad)}$, to that of the ZnP and H_2P references, $\Phi_{(reference)}$, and their lifetime, $\tau_{(reference)}$, allows determination of the rate constants for fluorescence deactivation, using eq 1:

$$k = \frac{[\Phi_{(reference)} - \Phi_{(dyad)}]}{[\tau_{(reference)}\Phi_{(dyad)}]} \quad (1)$$

These rate constants are listed in Table 2. The extremely fast rates of deactivation of the porphyrin singlet excited states (i.e., up to 10^{11} s^{-1}) infer very strong coupling between the porphyrin donor and C_{60} acceptor moieties.

1.5.2. Fluorescence Lifetime Data. The fluorescence decays of the dyads in toluene following excitation at 550 nm were monitored at 615 nm. For **H_2P−Az−C_{60}** dyads **4a** and **4b**, the fluorescence decay profiles were biexponential, with short-lived (i.e., 0.60 ns for **4a** and 0.79 ns for **4b**) and long-lived components (ca. 1.5 ns); the latter agrees well with the measured fluorescence lifetime of the C_{60} reference[15] (see Figure S9, Supporting Information, for time-resolved decays of the ZnP reference and dyad **4a)**. The singlet excited-state lifetimes for **4a** and **4b** in toluene measured by pump−probe experiments were 0.56 and 0.72 ns (see Table 2). For ZnP dyads **5a** and **5b** in toluene, only the long-lived component was observed, since the fast decays were shorter than 100 ps, outside the detection range of the instrumentation used in these studies. The value of 0.11 ns for **5b** in toluene given in Table 2 is at the limit of detection of the instrumentation. In parallel experiments, the fluorescence decays of all the dyads were measured at 725 nm, corresponding to C_{60} fluorescence, where again values of ~1.5 ns were observed. Thus, the short-lived component corresponds to the quenched H_2P fluorescence, while the longer component corresponds to the intrinsic unquenched C_{60} fluorescence. As expected from previous studies, no evidence for C_{60} fluorescence was found for any of the dyads in more polar solvents, THF and BzCN, where the singlet-state deactivation of the dyads fell within the time resolution of the apparatus at Erlangen, which is ~0.1 ns.

In the related up-conversion measurements on free base dyads **4a** and **4b** at Tampere,[5f,k] samples were excited at 410 nm, and the emission at 655 nm was monitored in the picosecond time domain, corresponding to the first maximum of the **H_2P** emission. In toluene, a two-exponential decay for **4a** was observed, with components at 50 and 630 ps; similar experiments with **4b** also gave two decay components, at 30 and 520 ps (major component). The presence of two components could be explained by the presence of two isomeric dyads, i.e., *Z* and *E* isomers, or equilibrium between S_1 and some other state; we favor the latter explanation, as discussed below. On the basis of other data discussed below, the longer major component is assigned to intramolecular singlet−singlet energy transfer from H_2P to the C_{60} moiety. Experiments at longer time domains, where the C_{60} fluorescence would have been observed (see above), were not performed. For dyad **4a** in benzonitrile (BzCN), fitting of the decay data at 655 nm required three exponentials, of which the major component of 160 ps is considered reliable; from similar experiments with **4b** in BzCN, a 190 ps component could be reliably extracted. These values are attributed to intramolecular electron-transfer processes, confirmed by the pump−probe transient absorption studies summarized below. A significant long-lived decay component was detected in BzCN, whose lifetime greatly exceeded the time range of the instrument (up to 1.5 ns). A lifetime of at least 80 ns is estimated for this component. The nature of the associated decay pathway in BzCN is uncertain; one possibility is photochemical decomposition competitive with electron transfer.

Overall, the data for **4a** and **4b** from Erlangen and Tampere are in excellent agreement with respect to the major fluorescence decay components. The rate constant for photoinduced ET (i.e., charge separation) in THF and BzCN is $\geq 10^{10}$ s^{-1}, which is comparable to what we and others have seen with other types of P−C_{60} dyads.[22,23] The fact that the fluorescence decays upon long wavelength excitation are strictly monoexponential is a strong indication that only a single isomer of each azo-linked dyad is present, which we assume is the *trans* (*E*) isomer. We would expect even shorter fluorescence lifetimes for *cis* (*Z*) isomers, on the order of 10 ps, because of the closer proximity of the porphyrin and fullerene moieties.[22] All the data is consistent with intramolecular electron transfer as the dominant if not exclusive mechanism for deactivation of H_2P and ZnP singlet excited states in polar solvents, whereas singlet−singlet

energy transfer dominates in nonpolar solvents, as exemplified in this study by toluene.

1.5.3. Pump−Probe Studies: Transient Absorption Spectroscopy. Conclusive information about the nature of the phototransformations came from transient absorption spectroscopy. The excited-state properties of ZnP and H_2P are reference points for the interpretation of the features seen in the **ZnP−Az−C$_{60}$** (**5a** and **5b**) and **H$_2$P−Az−C$_{60}$** systems (**4a** and **4b**). The differential spectrum recorded immediately after a femtosecond 387 nm laser pulse for the ZnP reference is characterized by bleaching of the porphyrin Q-band absorption at 550 and broad absorption between 570 and 750 nm. As shown in earlier work,[24] these spectral features are indicative of the ZnP singlet excited state (E_S = 2.00 eV), formed with a rate constant of $\sim 1 \times 10^{12}$ s^{-1}. These features slowly decay ($k = 4.0 \times 10^8$ s^{-1}) to the energetically lower-lying triplet excited state (E_T = 1.53 eV) via intersystem crossing (ZnP triplet quantum yield, $\Phi_{triplet} = 0.88$).[24] The formation of penta-coordinated Zn in coordinating solvents, such as THF and benzonitrile, shifts the Q-band slightly to the red, to 565 nm, with respect to noncoordinating solvents (toluene and dichloromethane), without affecting the singlet formation and singlet−triplet intersystem crossing rates. Figure S10 (Supporting Information) illustrates differential absorption changes monitored upon femtosecond excitation of ZnP in benzonitrile. Similar differential absorption changes were recorded for the H_2P reference with minima at 518, 555, 595, and 655 nm. The S_1 decay for the porphyrin references, reflecting the singlet ($E_{Singlet}$ = 1.9 eV) to triplet ($E_{Triplet}$ = 1.4 eV) intersystem crossing process, is notably slower (9.9×10^7 s^{-1}) for H_2P than for ZnP (4×10^8 s^{-1}), consistent with a heavy atom effect in the latter material.

In femtosecond transient absorption measurements of the dyads, the strong singlet−singlet absorption of the ZnP and H_2P again grows in with a rate constant of $\sim 1 \times 10^{12}$ s^{-1} (see Figures S11 and S12, Supporting Information). This confirms the successful formation of the porphyrin singlet excited states despite the presence of C_{60}. Instead of the slow ISC dynamics exhibited by the ZnP and H_2P references, the singlet−singlet absorptions of the dyads **4** and **5** decay with accelerated dynamics. These singlet excited-state lifetimes, as determined from an average of first-order fits of the time/absorption profiles at various wavelengths, are listed in Table 2; some representative decay curves are given in Figures S13 and S14. The derived singlet excited-state lifetimes quantitatively match values derived from the steady-state and time-resolved fluorescence experiments. The singlet lifetimes can be employed to determine the singlet decay rates of the dyads k_d shown in Table 2 using eq 2;

$$k_d = 1/\tau_{(reference)} - 1/\tau_{(dyad)} \quad (2)$$

The transient absorptions observed for the dyads after completion of the singlet decay in all solvents bear no resemblance to those of porphyrin triplet excited states. Thus, following excitation of the dyads at 532 nm in toluene, fullerene singlet excited states with characteristic absorption features are generated on the picosecond time scale (data not shown). These features decay unimolecularly at 6.6×10^8 s^{-1} to form fullerene triplet states (E_T = 1.5 eV) showing characteristic absorption around 700 nm.[25] The spectral features of the C_{60} triplet excited state of **5b** are shown as an illustration in Figure 6. The differential absorption changes recorded immediately after an 8 ns pulse in toluene showed the same features as those observed at the end of the femtosecond experiments, in line with the proposed energy-transfer mechanism which ultimately generates fullerene triplet excited states. Thus, in toluene, the porphyrin antennae act as photosensitizers which transmit excitation to the covalently attached fullerene moiety. The overall triplet quantum yields for the dyads in toluene, as measured by our comparative method,[22,24,25] vary between 0.64 and 0.98, and are slightly lower than the value for the reference compound (Φ_T = 0.98).

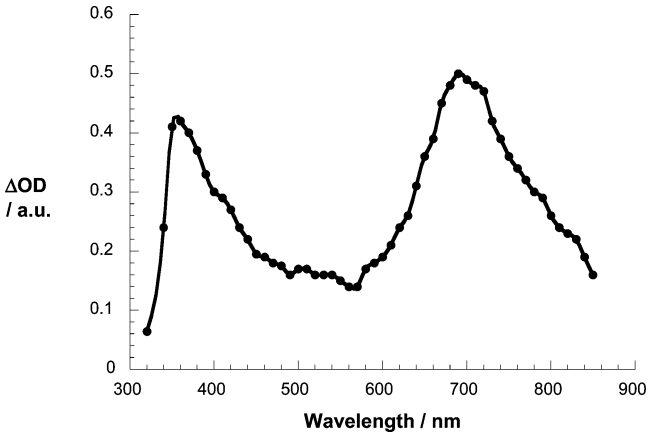

Figure 6. Differential absorption spectrum (visible, near-infrared) obtained upon nanosecond flash photolysis (532 nm) of dyad **5b** in nitrogen-saturated toluene. The spectrum corresponds to the C_{60} triplet excited state.[25]

When similar experiments were attempted at Tampere on **4a** and **5a** using 413 nm excitation, the samples underwent decomposition, as evidenced by new peaks in their absorption spectra.

The spectral changes observed upon excitation of the dyads in THF or BzCN are entirely different. Upon either 413 or 532 nm excitation of the dyads in THF and BzCN, transient absorption is observed at 650 and 1040 nm, characteristic of porphyrin radical cations and C_{60} radical anions, respectively,[22,23] clearly indicating formation of the charge-separated radical pair (CSRP) states **P$^{+\bullet}$−Az−C$_{60}^{-\bullet}$** and **ZnP$^{+\bullet}$−Az−C$_{60}^{-\bullet}$**. The transient absorption spectrum of dyad **5b** in THF is shown for illustration in Figure 7.

The decays of the transient absorption in THF at both 650 and 1040 nm in the nanosecond time range were cleanly

(23) (a) Kuciauskas, D.; Lin, S.; Seely, G. R.; Moore, A. L.; Moore, T. A.; Gust, D.; Drovetskaya, T.; Reed, C. A.; Boyd, P. D. W. *J. Phys. Chem.* **1996**, *100*, 15926. (b) DeGraziano, J. M.; Macpherson, A. N.; Liddell, P. A.; Noss, L.; Sumida, J. P.; Seely, G. R.; Lewis, J. E.; Moore, A. L.; Moore, T. A.; Gust, D. *New J. Chem.* **1996**, *20*, 839. (c) Liddell, P. A.; Sumida, J. P.; Macpherson, A. N.; Noss, L.; Seely, G. R.; Clark, K. N.; Moore, A. L.; Moore, T. A.; Gust, D. *Photochem. Photobiol.* **1994**, *60*, 537. (d) Liddell, P. A.; Kuciauskas, D.; Sumida, J. P.; Nash, B.; Nguyen, D.; Moore, A. L.; Moore, T. A.; Gust, D. *J. Am. Chem. Soc.* **1997**, *119*, 1400. (e) Gust, D.; Moore, T. A.; Moore, A. L. *Res. Chem. Intermed.* **1997**, *23*, 621. (f) Liddell, P. A.; Kodis, G.; De la Garza, L.; Bahr, J. L.; Moore, A. L.; Moore, T. A.; Gust, D. *Helv. Chim. Acta* **2001**, *84*, 2765. (g) Liddell, P. A.; Kodis, G.; Moore, A. L.; Moore, T. A.; Gust, D. *J. Am. Chem. Soc.*, **2002**, *124*, 7668. (h) Liddell, P. A.; Kodis, G.; Andreasson, J.; De la Garza, L.; Bandyopadhyay, S.; Mitchell, R. H.; Moore, T. A.; Moore, A. L.; Gust, D. *J. Am. Chem. Soc*. **2004**, *126*, 4803. (i) Liddell, P. A.; Kodis, G.; Kuciauskas, D.; Andreasson, J.; Moore, A. L.; Moore, T. A.; Gust, D. *Phys. Chem. Chem. Phys.* **2004**, *6*, 5509. (j) Terazono, Y.; Kodis, G.; Liddell, P. A.; Garg, V.; Gervaldo, M.; Moore, T. A.; Moore, A. L.; Gust, D. *Photochem. Photobiol.* **2007**, *83*, 464. (k) See also refs 3b and 4c.

(24) Guldi, D. M; Hirsch, A.; Scheloske, M., Dietel, E.; Troisi, A.; Zerbetto, F.; Prato, M. *Chem. Eur. J.* **2003**, *9*, 4968.

(25) Guldi, D. M.; Prato, M. *Acc. Chem. Res.* **2000**, *33*, 595.

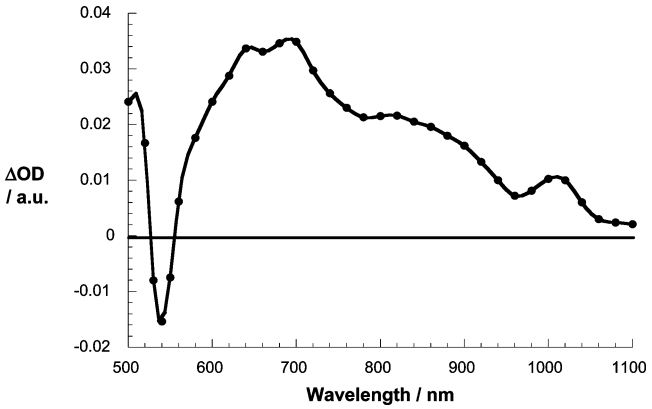

Figure 7. Differential absorption spectrum (visible and near-infrared) obtained upon nanosecond flash photolysis (532 nm) of $\sim 1.0 \times 10^{-5}$ M solutions of dyad **5b** in nitrogen-saturated THF with a time delay of 20 ns at room temperature. The spectrum corresponds to the charge-separated radical ion pair, $ZnP^{\bullet+}-Az-C_{60}^{\bullet-}$.

unimolecular, yielding the lifetimes of the CSRP states of these dyads shown in Table 2. The CSRP lifetimes in THF for *p*-tolyl dyads **4b** and **5b**, 435 and 290 ns, respectively, are about twice as long as those (175 and 145 ns, respectively) of 3,5-di-*tert*-butyl dyads **4a** and **5a**. The fact that the rate constants for charge recombination (BET) exceed those for charge separation in THF by ca. 3 orders of magnitude indicates that BET for these donor−acceptor systems takes place in the inverted region of the Marcus curve,[26,27] which has been repeatedly demonstrated for porphyrin−fullerene dyads.[6,7,22,23]

Studies in the ps time range on free base dyads **4a** and **4b** in BzCN with excitation at 413 nm gave somewhat different results. The decay component and time-resolved spectra (not shown) in the range 450−750 nm show readily discernible absorption features of the porphyrin radical cation as above. Two decay components in BzCN were measured for each dyad, of which the most significant are the long-lived components, 660 ps for **4a** and 1.2 ns for **4b**, which are assigned to decay of the CSRP states. The amounts of material available for these studies unfortunately precluded studies with excitation in the porphyrin Q-band region. Nonetheless, the CSRP states of **4b** are significantly longer-lived than are those of **4a** in both THF and BzCN, although the absolute decay rates differ by orders of magnitude for reasons which are not obvious at this time. This trend, at least for the free base dyads **4a** and **4b**, can be rationalized on the basis of the electrochemical data, since the oxidation potentials for the *p*-tolyl dyad **4a** is 30−60 mV lower than for the *tert*-butyl analogue **4b**. Thus, the thermodynamic driving force $-\Delta G^{\circ}_{CR}$ for the back electron transfer (BET) process for dyad **4b** is greater than for **4a**.

This is further support for charge recombination in the inverted region of the Marcus curve for these systems.[26,27] Smaller differences in oxidation potentials of the analogous ZnP dyads **5a** and **5b** are reflected by the smaller differences in BET rates measured in THF. Analogous charge recombination data for ZnP dyads **5a** and **5b** in BzCN are not available to compare with those in THF.

Table 3. Lifetimes of Charge-Separated Radical Pair States

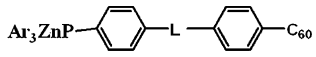

L	τ_{CR}, ns (THF)	Reference
	145	This work
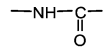	500	28
	660	28
	2800	28
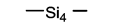	230-370	29
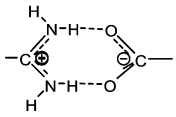	7900	30

2. Discussion

It is of interest to compare the photophysical properties of our azo-linked Zn dyad **5b** in THF with a series of **ZnP−linker−C$_{60}$** dyads studied by Imahori in which the identical donor and acceptor moieties are linked by rigid amide and acetylene spacers.[28] The relevant dyads are shown in Table 3. The rate constants for photoinduced charge separation in all these dyads are comparable: $1.0-1.2 \times 10^{10}$ s^{-1} for our system with a −N=N− linker compared with 1.3×10^{10} s^{-1}, 2.2×10^{10} s^{-1}, and 3.7×10^{10} s^{-1} for −NHCO−, −CONH− and −C≡C− linkers, respectively.[28] The rates of charge recombination (BET), however, are much more sensitive to the nature of the linker. In terms of the CSRP lifetimes in THF, these are 500 ns for −NHCO−, 660 ns for −CONH− and 2800 ns for −C≡C−, compared to our value of 290 ns for **5b** with a N=N linker. For further comparison, CSRP lifetimes of 250−400 ns in BzCN were recently reported for some novel tetrasilane-linked ZnP−C$_{60}$ dyads by Ito and co-workers,[29] while for a dyad in which Zn-tetraarylporphyrin and fullerene moieties are linked by hydrogen bonds, the charge-separated lifetime is 8 μs, the longest in this set of materials[30] (see Table 3 for structures and CSRP lifetime data). It is clear that the nature of the linker plays a critical role in mediating the BET process between the chromophores. Since the distances between the porphyrin and C$_{60}$ moieties are not significantly different in Imahori's dyads and our azo-linked dyad *trans*-**5b**, as well as the other dyads mentioned above, the large differences in the CSRP lifetimes are tentatively attributed to differences in the mechanism of BET. Since the azobenzene-linked dyad **5b** is completely conjugated, through-bond interactions by an electron exchange mechanism are facilitated for both charge separation and charge

(26) Marcus, R. A. *J. Chem. Phys.* **1956**, *24*, 966.
(27) For discussion of the low reorganization energy associated with C$_{60}$, see: (a) Imahori, H.; Hagiwara, K.; Akiyama, T.; Aoki, M.; Taniguchi, S.; Okada, T.; Shirakawa, M.; Sakata, Y. *Chem. Phys. Lett.* **1996**, *263*, 545.(b) Guldi, D. M.; Fukuzumi, S. In *Fullerenes, From Synthesis to Optoelectronic Properties*; Guldi, D. M., Martin, N., Eds.; Kluwer Academic Publishers: Dordrecht, 2002; pp 237−265, in addition to many of the articles in refs 22 and 23.
(28) Imahori, H.; Yamada, H.; Guldi, D. M.; Endo, Y.; Shimomura, A.; Kundu, S.; Yamada, K.; Okada, T.; Sakata, Y.; Fukuzumi, S. *Angew. Chem., Int. Ed.* **2002**, *41*, 2344.
(29) Shibano, Y.; Sasaki, M.; Tsuji, H.; Araki, Y.; Ito, O.; Tamao, K. *J. Organomet. Chem.* **2007**, *692*, 356.
(30) Sanchez, L.; Sierra, M.; Martín, N.; Myles, A. J.; Dale, T. J.; Rebek, J., Jr.; Seitz, W.; Guldi, D. M. *Angew. Chem., Int. Ed.* **2006**, *45*, 4637.

recombination processes. There is abundant evidence that electron exchange through double bonds is promoted over the same process through triple bonds because of differences in energies of lowest unoccupied molecular orbitals.[31] Thus, it is not at all surprising that BET in Imahori's acetylene-linked system is much slower than in our azo-linked dyad. Studies of the temperature dependence of the BET dynamics in our materials should provide insight into the mechanism of the process.

There is no evidence that photoinduced *cis*−*trans* isomerization is occurring in these azo-linked dyads, indicating that intramolecular energy- and electron-transfer processes are much faster than photoisomerization following electronic excitation, although as mentioned above some evidence of photochemical decomposition on continued irradiation was noted. Thermal and photochemical decomposition of the azo dyads does not seem to occur on extended storage in the dark or on limited exposure to long wavelength light, but it does occur upon continued exposure to shorter-wavelength visible light at 413 nm.

3. Summary

In summary, the first series of azobenzene-linked porphyrin−fullerene dyads have been synthesized, and their photophysical properties have been thoroughly investigated. While no major differences are observed in rate constants for photoinduced intramolecular electron transfer (charge separation) in comparison with closely analogous dyads with amide and acetylenic linkers, as well as other structural motifs, BET rates are significantly faster in our azo-linked dyads. In all cases, rates of BET are slow relative to rates of charge separation, by as much as 4 or 5 orders of magnitude. This is consistent with the conclusion that charge recombination in all of these dyads is occurring in the Marcus-inverted region.[26,27]

4. Experimental Section

4.1. General Procedures. Unless specified, all reagents and solvents were purchased from commercial sources and were used as received. $^3He@C_{60}$ was obtained from Prof. M. Saunders and Prof. R. J. Cross at the Chemistry Department of Yale University. Dry dichloromethane and toluene were freshly distilled over calcium hydride. Moisture-sensitive liquids and solutions were transferred by syringes and introduced into reaction vessels through rubber septa. All the reactions were stirred magnetically unless noted otherwise. The progress of the reactions was monitored by thin-layer chromatography (TLC) whenever possible. TLC was performed using precoated glass plates (Silica gel 60, 0.25 mm thickness) containing a 254 nm fluorescent indicator.

4.2. General Procedure for MnO_2-Mediated Oxidative Coupling Reaction. The aminoporphyrin (**1a**, **1b**) (0.2 mmol) and aminoacetal **2** (0.6 mmol) were dissolved in dry toluene (100 mL) and heated at reflux in a round-bottom flask equipped with a Dean−Stark setup. MnO_2 was added to the solution portion batchwise (each batch 0.1 mmol, 1.2 mmol total) until all the aminoporphyrin was consumed. The purple solution was filtered through a pad of celite to remove the solid, and the residue was washed thoroughly with dichloromethane. The solvent was removed *in vacuo*, and the crude product was subjected to the deprotection procedure directly without further purification. The *p*-tolyl product was purified for analytical purposes. The residue was dissolved in dichloromethane (20 mL), trifluoroacetic acid (1 mL), and water (4 mL). The biphasic mixture was stirred at room temperature overnight. The solution was diluted with dichloromethane and washed with saturated sodium bicarbonate until the organic phase became completely purple. The organic layer was separated and dried over Na_2SO_4. The solvent was removed *in vacuo*, and the residue was purified by column chromatography. Column chromatography (SiO_2, hexanes/CH_2Cl_2 = 2:1 to 1:2) to give the desired product **3a**, **3b** in 50−60% yield.

4.3. Me-TPP-azo-Ph-acetal 3a (R = R_1): ^{1}H NMR (400 MHz, $CDCl_3$), Figure S16: δ 8.89−8.84 (m, 8H), 8.40 (d, 2H, J = 8.3 Hz), 8.33 (d, 2H, J = 8.3 Hz), 8.13 (m, 8H), 7.77 (d, 2H, J = 7.8 Hz), 7.57 (d, 6H, J = 8.3 Hz), 5.54 (s, 1H), 3.85 (d, J = 11.2 Hz, 2H), 3.74 (d, J = 11.2 Hz, 2H), 2.70 (s, 9H), 1.34 (d, 3H, J = 18.4 Hz), 0.83 (d, 3H, J = 18.4 Hz), −2.74 (s, 2H) MALDI-TOF Mass: calcd 875.4 $C_{59}H_{51}N_6O_2$ $[M + H]^+$, found 875.0.

4.4. Me-TPP-azo-Ph−CHO (3a, R = CHO): ^{1}H NMR (400 MHz, $CDCl_3$), Figure S17: δ 10.11 (s, 1H), 8.93−8.89 (m, 8H), 8.43 (d, 2H, J = 8.3 Hz), 8.35 (d, 2H, J = 8.3 Hz), 8.15 (d, 2H, J = 8.3 Hz) 8.12 (d, 6H, J = 7.8 Hz), 8.06 (d, 2H, J = 8.3 Hz), 7.56 (d, 6H, J = 7.8 Hz), 2.69 (s, 9H), −2.79 (s, 2H). MALDI-TOF Mass: calcd 789.3 $C_{54}H_{41}N_6O$ $[M + H]^+$, found 789.0.

4.5. *tert*-Bu-TPP−azo-Ph−CHO (3b, R = CHO): ^{1}H NMR (400 MHz, $CDCl_3$), Figure S18: δ 10.14 (s, 1H), 8.93−8.87 (m, 8H), 8.43−8.35 (m, 4H), 8.19 (d, 2H, J = 8.3 Hz), 8.10 (d, 2H, J = 8.3 Hz), 8.09−8.08 (m, 6H), 7.80−7.79 (m, 3H), 1.52−1.49 (m, 54H), −2.68 (s, 2H) MALDI-TOF Mass: calcd 1083.7 $C_{75}H_{83}N_6O$ $[M + H]^+$, found 1084.0.

4.6. Synthesis of Free Base Dyads 4a and 4b. Aldehyde **3a** or **3b** (0.02 mmol), *N*-methylglycine (9 mg, 0.11 mmol), and C_{60} (72 mg, 0.1 mmol) were dissolved in dry toluene (30 mL) under N_2 atmosphere; the mixture was heated at reflux for 6 h. The crude product was directly purified by column chromatography (SiO_2, hexane/toluene = 4:1 to 1:2). The desired product was obtained in ∼60% yield.

4.7. Dyad 4a: ^{1}H NMR (400 MHz, $CDCl_3$), Figure S19: δ 8.88−8.85 (m, 8H), 8.29 (m, 4H), 8.14 (d, 2H, J = 7.6 Hz), 8.08 (d, 6H, J = 7.6 Hz), 7. 85 (br, 2H), 7.55 (d, 6H, J = 7.6 Hz), 4.75 (br, 2H), 4.00 (br, 1H), 2.76 (s, 3H), 2.70 (s, 9H), −2.78 (s, 2H). MALDI-TOF Mass calcd 816.4 $C_{56}H_{46}N_7$ $[M - C_{60} + H]^+$, found 816.0 **Dyad 4b:** ^{1}H NMR (400 MHz, $CDCl_3$), Figure S20: δ 8.89−8.85 (m, 8H), 8.29 (m, 4H), 8.17 (d, 2H, J = 8 Hz), 8.08 (s, 6H), 7.97 (br, 2H), 7.80 (s, 3H), 4.81 (m, 2H), 4.08 (d, 1H, J = 10 Hz), 2.83 (s, 3H), 1.53−1.52 (m, 54H), −2.75 (s, 2H). MALDI-TOF Mass calcd 1112.7 $C_{77}H_{88}N_7$ $[M - C_{60} + H]^+$, found 1113.0.

4.8. Zn Dyads 5a and 5b. Dyad **4a** or **4b** (0.01 mmol) was dissolved in CH_2Cl_2 (10 mL) and heated at reflux. A solution of zinc acetate (100 mg) in MeOH (1 mL) was added, and heating was continued for 30 min. The mixture was cooled to room temperature and extracted with water (10 mL). The organic layer was separated, dried over $MgSO_4$, and passed through a short silica gel plug. The product **5a** or **5b** was obtained in ∼90% yield. **Dyad 5a:** ^{1}H NMR (400 MHz, $CDCl_3$), Figure S21: δ 8.98−8.93 (m, 8H), 8.31−8.27(m, 4H), 8.15 (d, 2H, J = 8.3 Hz), 8.09−8.05 (m, 8H), 7.57−7.53 (m, 6H), 4.71−4.64 (m, 2H), 3.93 (d, 1H, J = 9.1 Hz), 2.79 (s, 3H), 2.71 (s, 9H), MALDI-TOF Mass calcd 877.3 for $C_{56}H_{43}N_7Zn$ $[M - C_{60}]^+$, found 877.0 **Dyad 5b:** ^{1}H NMR (400 MHz, $CDCl_3$), Figure S22: δ 8.89−8.85 (m, 8H), 8.29 (m, 4H), 8.17−8.08 (m, 8H), 7.97 (br, 2H), 7.80 (s, 3H), 4.81 (m, 2H), 4.08 (d, 1H, J = 10 Hz), 2.83 (s, 3H), 1.53−1.52 (m, 54H), MALDI-TOF Mass calcd 1173.6 for $C_{77}H_{85}N_7Zn$ $[M - C_{60}]^+$, found 1174.

4.9. Electrochemical and Photophysical Measurements. Descriptions of the electrochemical and photophysical experimental methods are found in the citations to previous studies by Echegoyen, Guldi, and Lemmetyinen, respectively, as well as those given in our previous collaborative publications (see ref 22).

Acknowledgment. We are grateful to the National Science Foundation (Grant CHE 0097089) and the Petroleum Research Fund (Grant PRF 40362-AC4) administered by the American Chemical Society for support of this research.

(31) Seybold, P. G.; Gouterman, M. *J. Mol. Spectrosc.* **1969**, *31*, 1.

We also thank Prof. Phil S. Baran (The Scripps Research Institute) for valuable suggestions regarding the synthesis of the new dyads. Components of this work at NYU were conducted in a Shared Instrumentation Facility constructed with support from Research Facilities Improvement Grant C06 RR-16572 from the National Center for Research Resources, National Institutes of Health. D.I.S. and K.L. acknowledge Grant MRI-0116222 from the National Science Foundation for the purchase of new NMR spectrometers at NYU. D.M.G. acknowledges partial support from the SFB 583, DFG (GU 517/4-1), FCI, and the Office of Basic Energy Sciences of the U.S. Department of Energy. L.E. and A.P. greatly appreciate financial support from the United States National Science Foundation (Grant CHE-0509989).

Supporting Information Available: Cyclic voltammograms (CV) of compounds **3**, **4b**, **5b**; differential pulse voltammetry (DPV) of compounds **3**, **4b**, **5b**; time-resolved fluorescence decay of ZnP reference and dyad **4a**; differential absorption spectra and time-absorption profiles of ZnP reference and dyads **4a**, **5a**, and **5b**; ^{3}He NMR of compound **4b**; ^{1}H NMR spectra of **3**, **4**, **5**. This material is available free of charge via the Internet at http://pubs.acs.org

JA074684N